JOURNAL OF SPACECRAFT AND ROCKETS
Vol. 36, No. 5, September–October 1999

Asymmetric Divert Jet Performance of a Supersonic Missile: Computational and Experimental Comparisons

B. Srivastava*
Raytheon Company, Tewksbury, Massachusetts 01876

Computational fluid dynamics (CFD) predictions are compared with the wind-tunnel tests for a missile consisting of ogive-nose cylindrical body, four wings, and four in-lined tail panels at nominal supersonic Mach numbers 2, 3, 4, and 5 and at angles of attack ranging from 0 to 35 deg with and without a lateral jet thruster with thrust ratios of 1 and 4. Comparisons also include roll angles that lead to asymmetric missile configuration with the thruster jet. Excellent comparisons of the predicted normal-force, side-force, pitching-moment, yawing-moment, and rolling-moment coefficients with the measured data are shown. CFD-computed flowfield then is utilized to show that the lateral thruster jet effectiveness diminishes as the jet thruster is gradually rolled toward the windward side of the missile. Flow physics associated with this phenomenon and possible mechanisms to alleviate this effect are discussed.

Nomenclature

C_{lm} = rolling-moment coefficient, $M_x/(q \cdot S \cdot X_{\text{ref}})$
C_m = pitching-moment coefficient, $M_y/(q \cdot S \cdot X_{\text{ref}})$
C_N = normal-force coefficient, $(N/q \cdot S)$, airframe only
C_Y = side-force coefficient, $F_Y/(q \cdot S)$
C_{Ym} = yawing-moment coefficient, $M_z/(q \cdot S \cdot X_{\text{ref}})$
d_p = pressure differential
F_Y = side force, lb
M = freestream Mach number
M_x = rolling moment
M_y = pitching moment
M_z = yawing moment
N = normal force, lb
P = pressure, lb/ft^2
q = dynamic pressure, $\frac{1}{2}\rho v^2$
S = missile cross-sectional area, ft^2
T = jet thrust, lb
v = velocity, ft/s
α = angle of attack, deg
γ = ratio of specific heats
ρ = density
ϕ = azimuth angle, deg

Subscripts

inf = freestream condition
jet = condition with jet (excluding jet thrust coefficient)
no-jet = condition with no jet
ref = reference length for normalization

Introduction

FOR short-range air-to-air missiles, high maneuver requirements at launch and in the homing phase (terminal engagement) are necessary for tactical advantage in air combat engagements. Missile maneuvers up to 60–90 deg may be required to defend against threats. Conventional methods of improving the aerodynamic control maneuver are limited by the weight and drag requirements of the overall missile. Advanced concepts are under study for enhancing the high angle-of-attack performance of the current and next-generation missiles. Reaction control jets may be ideal for such applications because of their rapid response time as well as their ability to perform at all speeds and altitudes. Additional benefits include reduced size of wings and fins that can overcome the weight penalty of the reaction control system. Similar benefits are likely for a surface-to-air combat scenario.

A successful effort based on the reaction control jets, however, must develop a rational basis for design factors such as the jet size, locations, number of jets, thrust levels, effect of jet temperature, jet angle, and, most importantly, its interaction with the missile external flow. The problem of jet interaction with the external flow, under conditions of varying flight numbers and angles of attack, is extremely complex, and an understanding of this interaction is important to achieve optimal missile performance. A large volume of experimental and analytical studies related to lateral jets, dating back to the 1960s, are available in the literature. However, in spite of these studies, numerous related issues need to be addressed.

Because of the complexity of the flow involved in this interaction process, a viable approach to address some of these issues is to combine the wind-tunnel testing and computational fluid dynamics (CFD) simulations to evolve a validated design and analysis tool. The former provides a valuable database for CFD validation whereas the latter provides a means for parametric design evaluation. This approach also offers a methodology to synthesize the physical complexity of the flow in an effort to identify the key controlling parameters by sequentially increasing the physical complexity of the model in a CFD simulation. At Raytheon, our design team has adopted this approach, i.e., scale-model testing, CFD validation, and design tradeoff studies using validated CFD tools.

Our previous efforts for this topic dealt with CFD simulation and validation for a symmetric missile with wings and tail panels at 17 flow conditions corresponding to the wind-tunnel tests.[1–4] More specifically, validations were performed at a nominal $M = 3.94$, $\alpha = 2$–25 deg, three different wing planforms, and lateral jet thrust ratios of 1 and 4. These studies show excellent comparisons of the CFD predicted normal-force and pitching-moment coefficients with the wind-tunnel data. For symmetric cases, however, a need exists to extend the validation range to other supersonic Mach numbers, e.g., $M = 2$–5 and higher angles of attack, e.g., $\alpha = 75$ deg. Likewise, validations for asymmetric missile orientations for similar Mach number and angle of attack ranges need to be performed to establish a credible design and analysis tool.

The present paper deals with several additional validation studies corresponding to the wind-tunnel tests, specifically for asymmetric missile orientations with and without lateral jets. Sixteen symmetric wind-tunnel cases and an additional 17 asymmetric wind-tunnel cases are compared with the CFD predictions. The computational results with reaction jets then are analyzed to show that the reaction jets do not perform well in the windward orientation. In this orientation, the intense interaction between the incoming freestream and the jet causes a blockage effect that wipes out the normal forces

Received 29 June 1998; revision received 20 December 1998; accepted for publication 29 January 1999.

*Senior Design and Development Engineer, Electronics System Division; currently Lead Engineer, General Electric Aircraft Engine, Lynn, MA 01910. Senior Member AIAA.

on the windward wing and tail panels, leading to deterioration of missile performance. Possible design variations that can circumvent this deficiency associated with the reaction jets are outlined.

The paper is divided in several sections. The Background section briefly outlines the previous work in this area using CFD approaches. Then, the details of the computational methodology, geometry, grid-related issues, and boundary conditions of the CFD applications are discussed. Our previous paper[2] presented a large number of validation cases with the wind-tunnel data with and without divert thrusters. Further validation cases at several Mach numbers for symmetric and asymmetric missile configurations are discussed in the section on Comparison with Wind-Tunnel Tests. The bulk of the technical discussion related to the effect of divert thruster location on missile performance occurs in the Discussion section. Finally, a summary and conclusions based on these computational studies are presented.

Background

The topic of jet interaction with an external supersonic flow dates back to the mid-1960s,[5,6] when much generic experimental data were generated and related correlation techniques were developed. Emergence of hypersonic interceptors, maturity of CFD, and the advent of supercomputers revived these activities in the late 1980s.[7–11] Several investigators have performed CFD studies for the fundamental problem of jet interaction in relation to adaptive gridding,[12] turbulence models,[13] grid refinements,[14] and the impact of artificial viscosity.[12] These studies range from Euler[15] to Navier–Stokes computations.[16] We make particular reference to the studies reported by Dash et al.[16] and York et al.[10] because much of the current CFD effort is derived from their mature technical expertise in this area. Further details of the methodology and related research work can be obtained from the references cited.

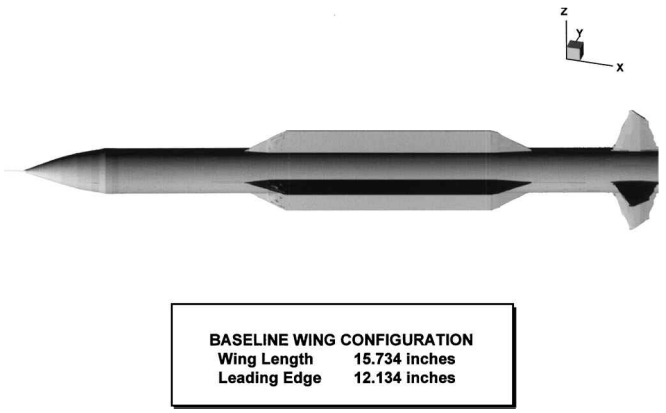

Fig. 1 Three-dimensional view of a generic missile.

Although a vast number of numerical studies have been performed using controlled jet interaction studies for methodology development, efforts to simulate missile surfaces have been rather limited. More recently, Chan et al.[17] performed a series of studies that led to the simulation of a full missile surface with control surfaces and jet interaction. Qin and Foster[18] also performed similar studies using a Navier–Stokes approach for an inclined jet on an ogive/cylinder body. These results depict the remarkable flow details obtained using CFD approaches, which ultimately result in making judicious choices for flight vehicle design and further wind-tunnel testing. Srivastava[3] performed full Navier–Stokes (FNS) studies for generic missile bodies with and without leeward and windward jets but without wing or tail panels. Comparisons with the wind-tunnel data, however, was not direct because the tests were conducted with tail panels but computations were performed without tail. Removal of the tail load from the wind-tunnel data by an approximate method introduced uncertainties that were not fully quantified. This deficiency in the CFD model was eliminated later by Srivastava,[4] showing direct comparison of the CFD predictions with the wind-tunnel data by modeling all geometric aspects of the wind-tunnel missile geometry and the divert thruster.

Computational Methodology

PARCH,[10] which is a FNS code with plume/missile airframe steady-flow predictive capability, is being used for our current studies. The PARCH code utilizes formulations based on the NASA Ames Research Center aerodynamic code and the Arnold Engineering Development Center propulsive extension, PARC. This code is particularly suited for missile surfaces because of its grid patching capability, which is useful for treating embedded surfaces in a flowfield. Patching, which is accomplished in mapped computational coordinates, is automatically constructed from boundary inputs. Boundary conditions are applied along the outer computational boundaries and relevant embedded surfaces. The code utilizes diagonalized Beam–Warming numerics with matrix-split finite rate chemistry. Several versions of the K-E turbulence model

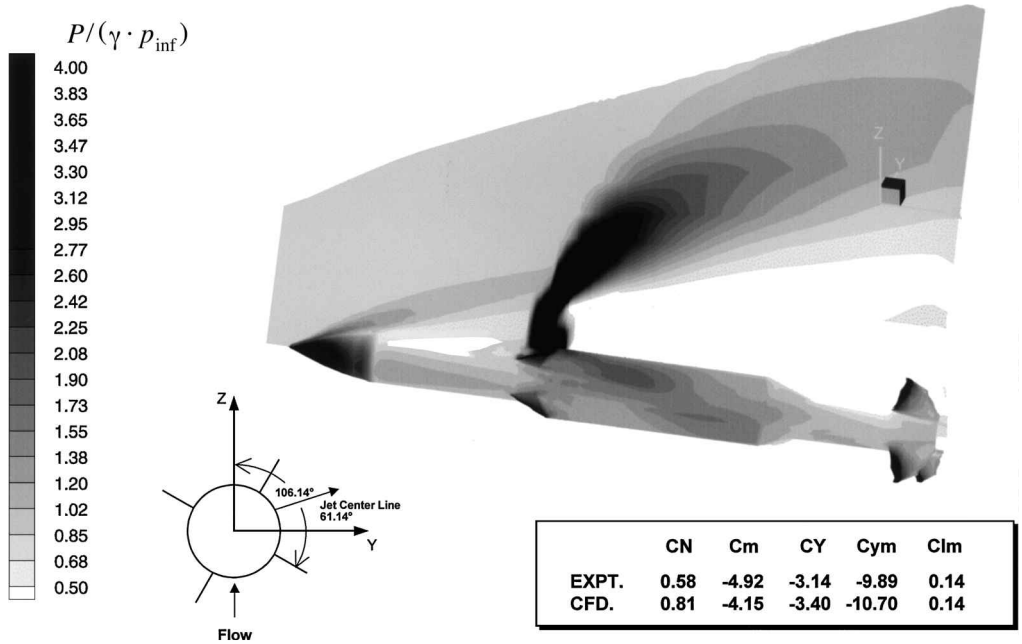

Fig. 2 Pressure distribution on jet center plane and missile surfaces for a leeward jet: flow Mach number, 3.94; angle of attack, 9.4 deg; ϕ, 106.14 deg; and jet thrust, 175 lb.

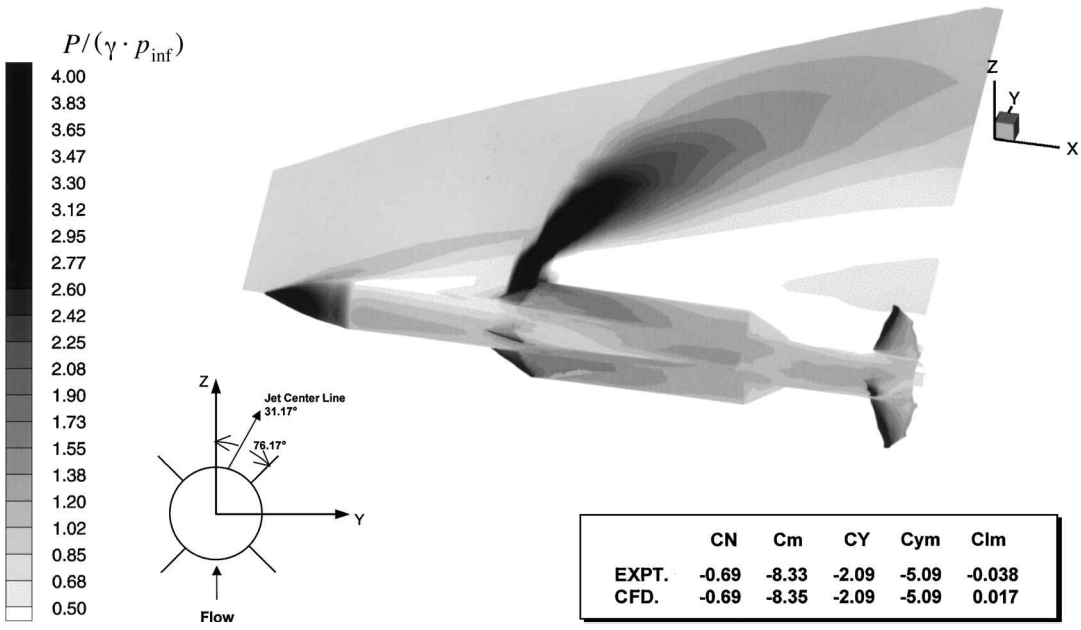

Fig. 3 Pressure distribution on jet center plane and missile surfaces for a leeward jet: flow Mach number, 3.94; angle of attack, 9.0 deg; ϕ, 76.17 deg; and jet thrust, 175 lb.

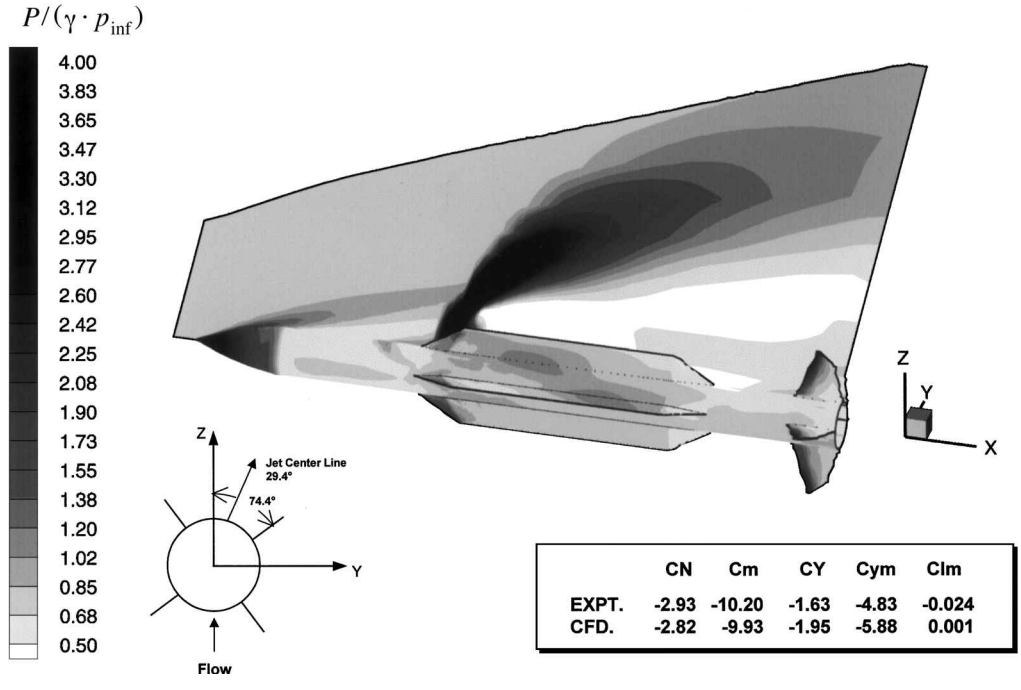

Fig. 4 Pressure distribution on jet center plane and missile surfaces for a leeward jet: flow Mach number, 3.94; angle of attack, 2.3 deg; ϕ, 74.4 deg; and jet thrust, 175 lb.

that were developed specifically for jet interaction and propulsive studies are available in the code. We are using the capped low Reynolds number formulation of Chien's K-E model[16] for these simulations. Further details of the code capability can be found elsewhere.[10]

Typical boundary approaches for the current application (supersonic flows) are specified supersonic freestream conditions at the inlet and outer boundaries. Extrapolation procedures are employed at the exit boundary. Surface conditions are appropriate to viscous flows with adiabatic wall condition.

Surface jet boundary condition is the specified jet nozzle supersonic exit conditions. The circular area of the jet in the wind-tunnel test is approximated by a square aperture in the CFD simulation.

Figure 1 shows a three-dimensional view of a generic missile geometry. The wing in Fig. 1 is the baseline configuration, which is 6.3 body diameters long and its leading edge starts at 4.85 body diameters from the missile nose. The jet thruster is located at 5.6 body diameters from the nose (additional details of this geometry can be obtained from Ref. 4).

CFD simulations were performed on a single grid consisting of $230 \times 51 \times 137$ axial, normal, and circumferential grid. A grid patching procedure was used to apply the relevant boundary conditions on the surfaces. All angles of attack for a given configuration were simulated on a single grid consistent with the minimum desired Mach number and maximum desired angle of attack. This allows us to minimize on the grid effort. The grids were generated through GRIDGEN, with geometry models developed within GRIDGEN.[19]

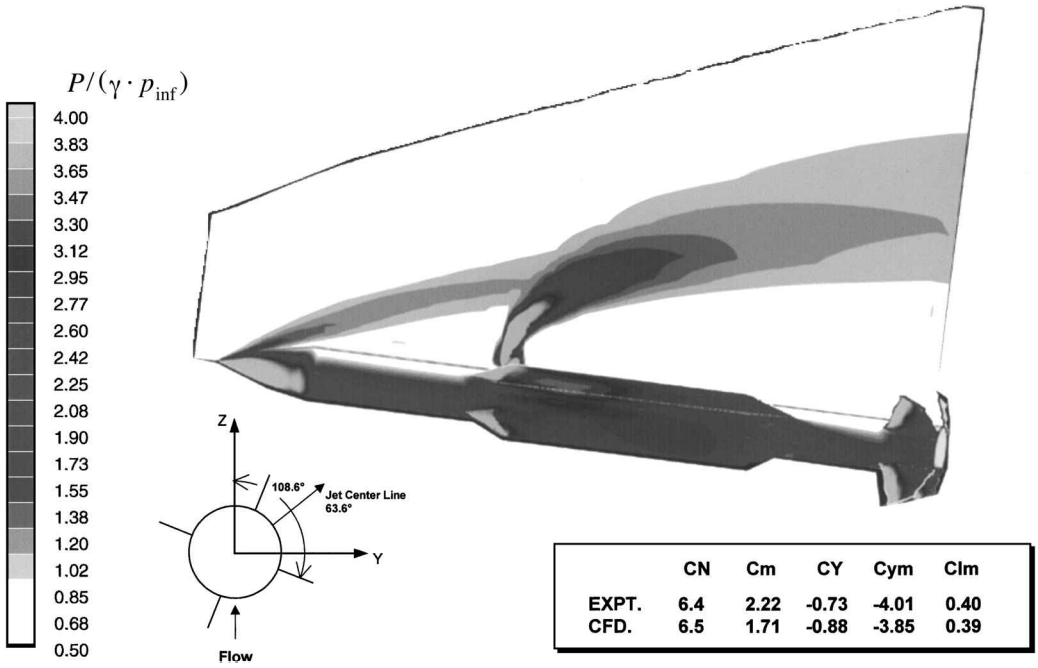

Fig. 5 Pressure distribution on jet center plane and missile surfaces for a leeward jet: flow Mach number, 3.94; angle of attack, 20 deg; ϕ, 108.6 deg; and jet thrust, 50 lb.

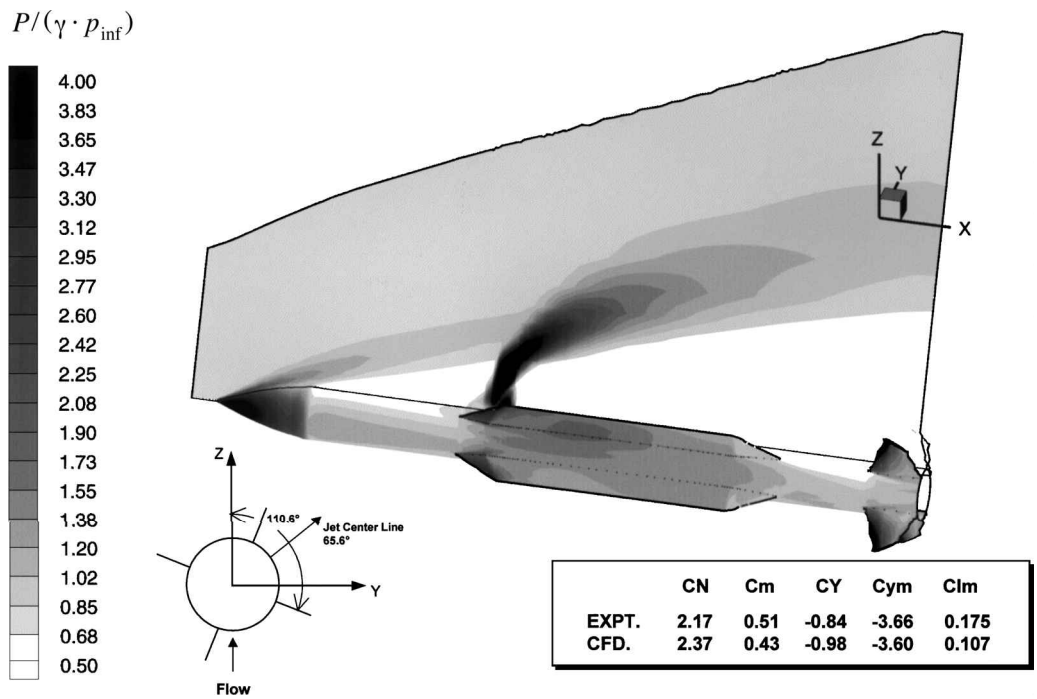

Fig. 6 Pressure distribution on jet center plane and missile surfaces for a leeward jet: flow Mach number, 3.94; angle of attack, 9.8 deg; ϕ, 110.6 deg; and jet thrust, 50 lb.

Our current studies for divert jet were performed for a nominal flow Mach number of 4 with an angle of attack ranging from 3 to 20 deg for several peripheral jet orientations.

Comparison with Wind-Tunnel Tests

Test Cases with Divert Jets

A large number of symmetric configuration test cases with divert jets were presented in our previous papers[2,3] showing excellent comparisons with the wind-tunnel data at a nominal $M = 4$ and $\alpha = 20$ deg. These comparisons were restricted to symmetric cases because of limited availability of the computing resources. It now is possible to simulate the asymmetric configuration using parallel processing on our six-processor Digital Alpha-8400 computing resources. These results are discussed next.

Asymmetric Cases

Asymmetric test cases were performed at the same nominal $M = 4.0$ and $\alpha = 20$ deg. Divert jet location was kept fixed with the missile rolled around its axis to achieve several different locations of the divert jet relative to the freestream. Some asymmetric cases were presented in Ref. 4, showing excellent comparisons with the experimental data. The results for other cases for a jet thrust of 175 and 50 lb are presented next.

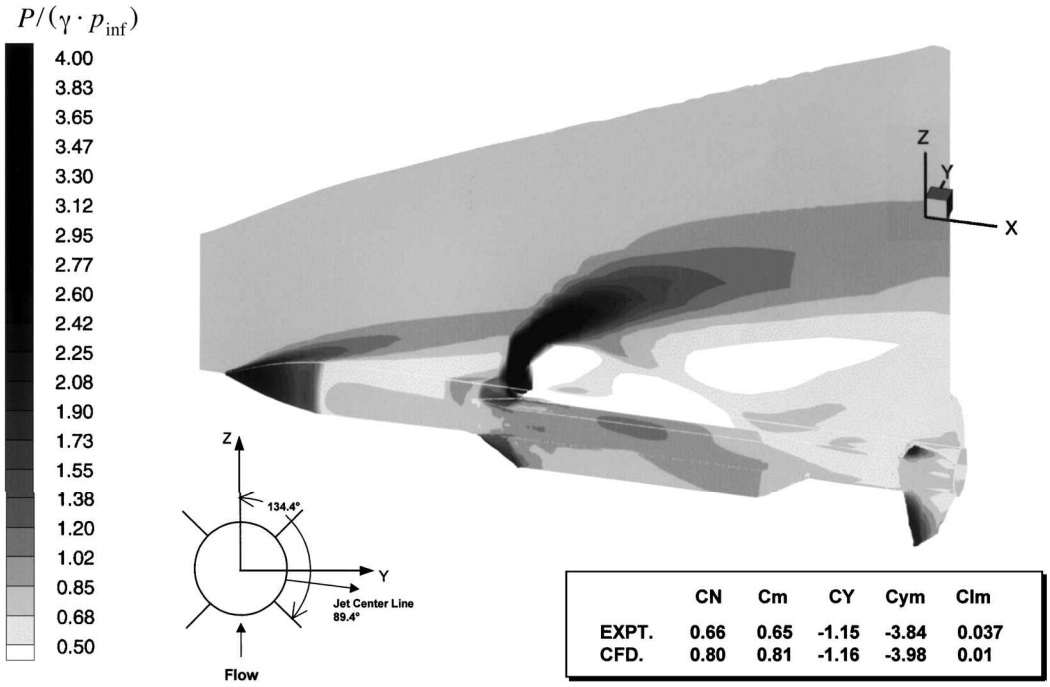

Fig. 7 Pressure distribution on jet center plane and missile surfaces for a side jet: flow Mach number, 3.94; angle of attack, 3.1 deg; ϕ, 134.4 deg; and jet thrust, 50 lb.

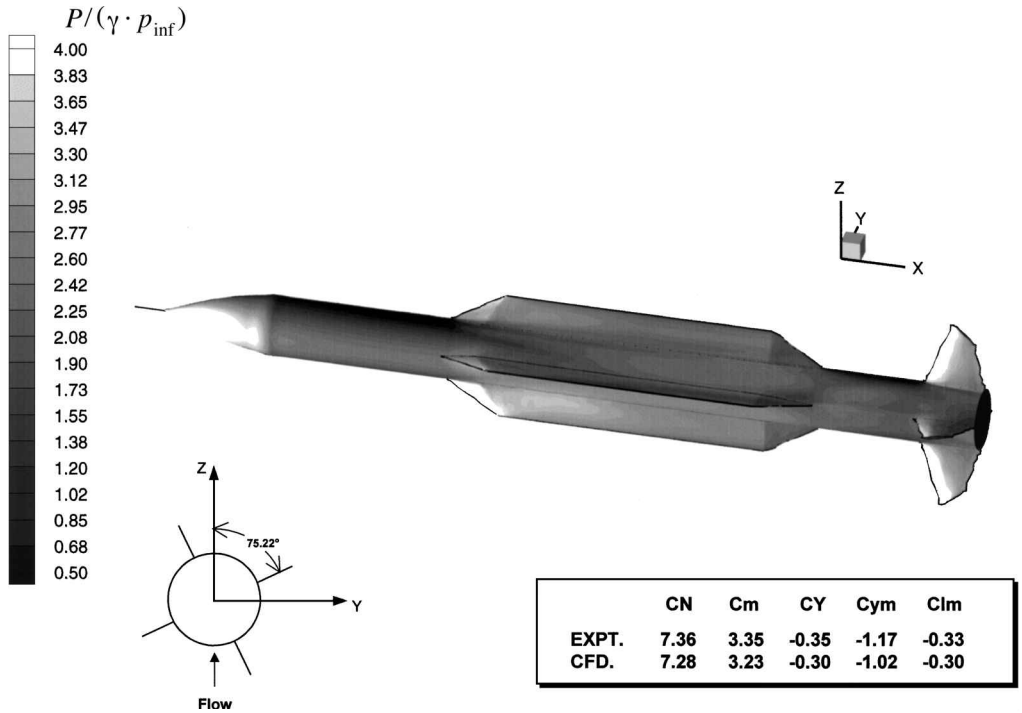

Fig. 8 Pressure distribution on missile surfaces for a supersonic asymmetric missile without jet: flow Mach number, 3.94; angle of attack, 20 deg; ϕ, 75.22 deg; and jet thrust, 50 lb.

Jet Thrust of 175 lb

Figures 2–4 show the comparisons of the CFD results with the wind-tunnel data for several roll angles, which represent divert jets in windward to leeward orientations. Figure 2 shows the computed results for a case that is rolled by about 106.14 deg clockwise from the vertical axis, such that the jet centerline makes an angle of 61.14 deg. The axis system shown in the figures is a right-hand system. This orientation is nearly an x configuration with a side jet orientation. Figure 2 shows the pressure distribution on a plane surface normal to the body and passing through the jet on the windward side and on the missile surfaces such as body, wing, and tail panels. Notice from this figure that because of the intense interaction between the jet and the freestream, the jet streams make a parabolic shape away from the missile surfaces. The table in Fig. 2 shows the comparison of the computed results with the wind-tunnel data for all force and moment coefficients. The excellent comparisons are noteworthy.

Figure 3 shows a computation with missile rolled by 76.17 deg such that the divert jet is now positioned at an angle of 31.17 deg from the vertical axis, a leeward thrust situation. The pressure

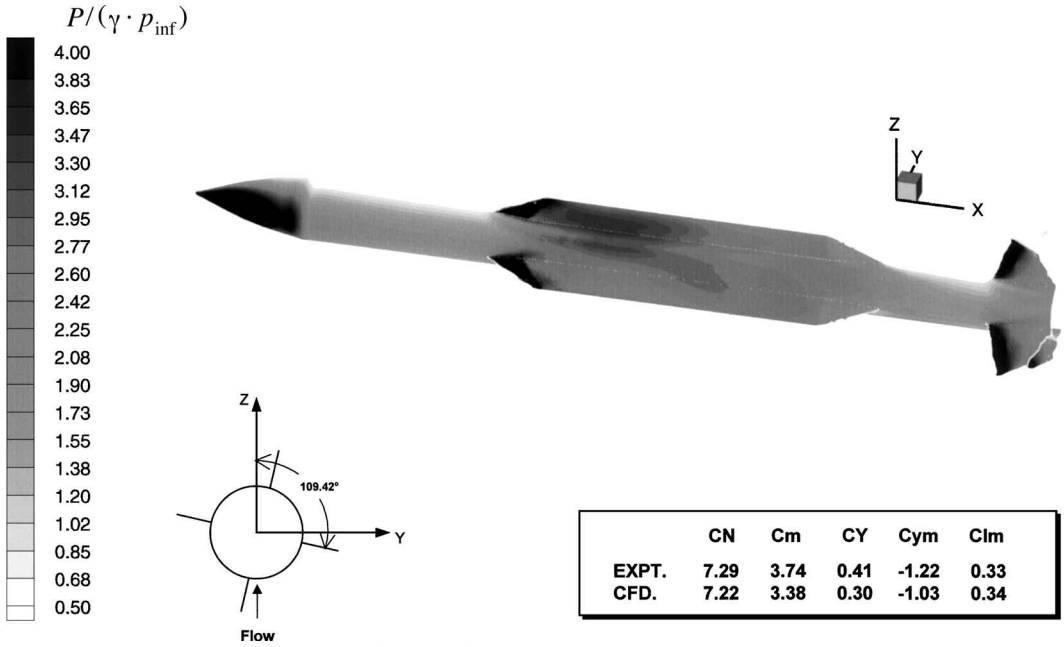

Fig. 9 Pressure distribution on missile surfaces for a supersonic asymmetric missile without jet: flow Mach number, 3.94; angle of attack, 20 deg; ϕ, 109.42 deg; and jet thrust, 50 lb.

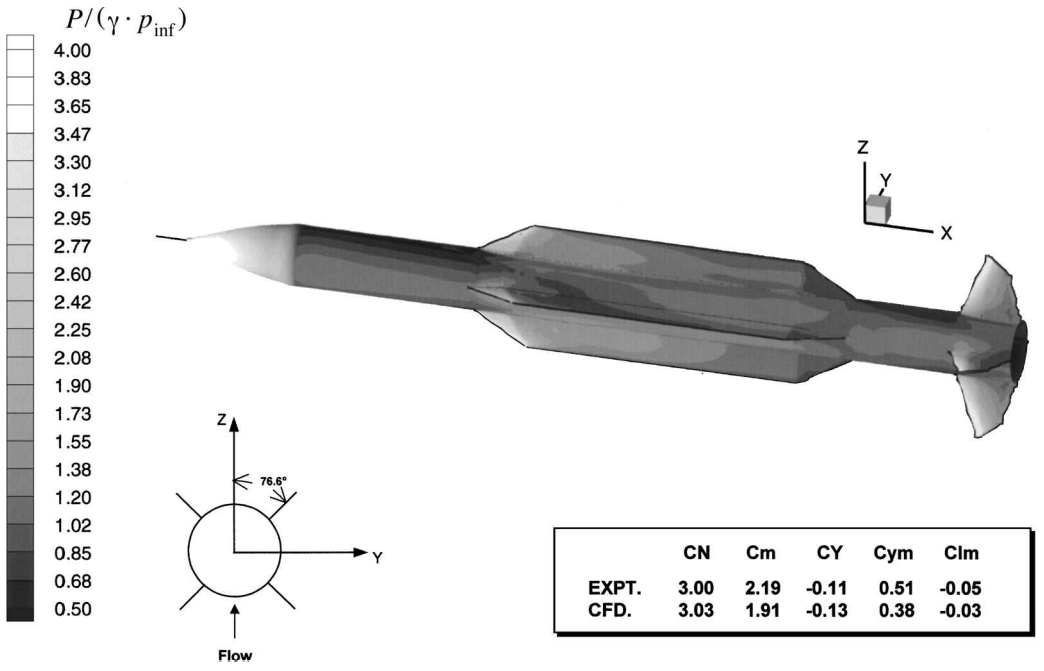

Fig. 10 Pressure distribution on missile surfaces for a supersonic asymmetric missile without jet: flow Mach number, 3.94; angle of attack, 9.93 deg; ϕ, 76.6 deg; and jet thrust, 50 lb.

contours are once again on a plane containing the jet and the missile surfaces. In this view, the observer is looking from the right side toward the positive y axis, between two wing panels showing pressure distribution on the surfaces. The computed force and moment coefficients once again show excellent agreement with the data.

Figure 4 shows one more case for this jet thrust level. This latter case is for nearly the same missile orientation and jet location as in Fig. 3 except that it is at a lower angle of attack. CFD results predict all coefficients very well except the rolling-moment coefficient. The main reason for this difference is the wind-tunnel balance accuracy for moment coefficients, which are projected to have measurement inaccuracies of ± 0.1. The wind-tunnel data shown in this figure are well below this limit.

In summary, for this jet thrust level the CFD predictions are excellent for a large number of missile roll angles and angles of attack at a supersonic $M = 4.0$. We are exploring available databases for other supersonic flow conditions.

Jet Thrust of 50 lb

Three more cases are discussed to show the effect of reduced jet thrust on missile performance as well as for CFD validation. Figures 5–7 show these results. The computational result in Fig. 5 is for an angle of attack of 20 deg and a missile roll angle orientation of 108.6 deg. In this missile orientation, the jet centerline makes an angle of 63.6 deg with the vertical axis. Notice that CFD predictions

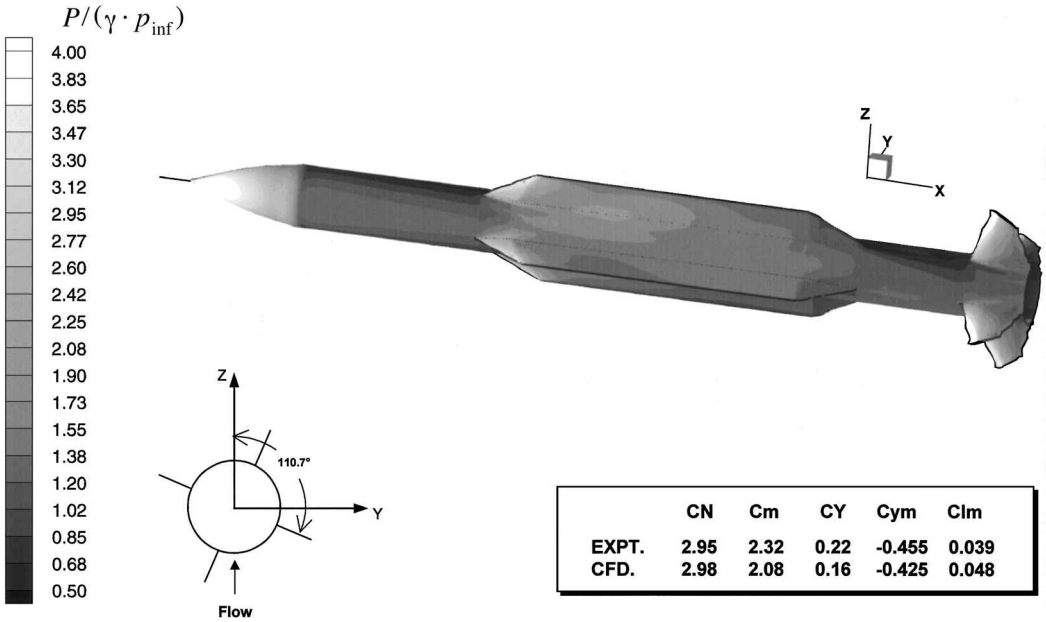

Fig. 11 Pressure distribution on missile surfaces for a supersonic asymmetric missile without jet: flow Mach number, 3.94; angle of attack, 9.92 deg; ϕ, 110.7 deg; and jet thrust, 50 lb.

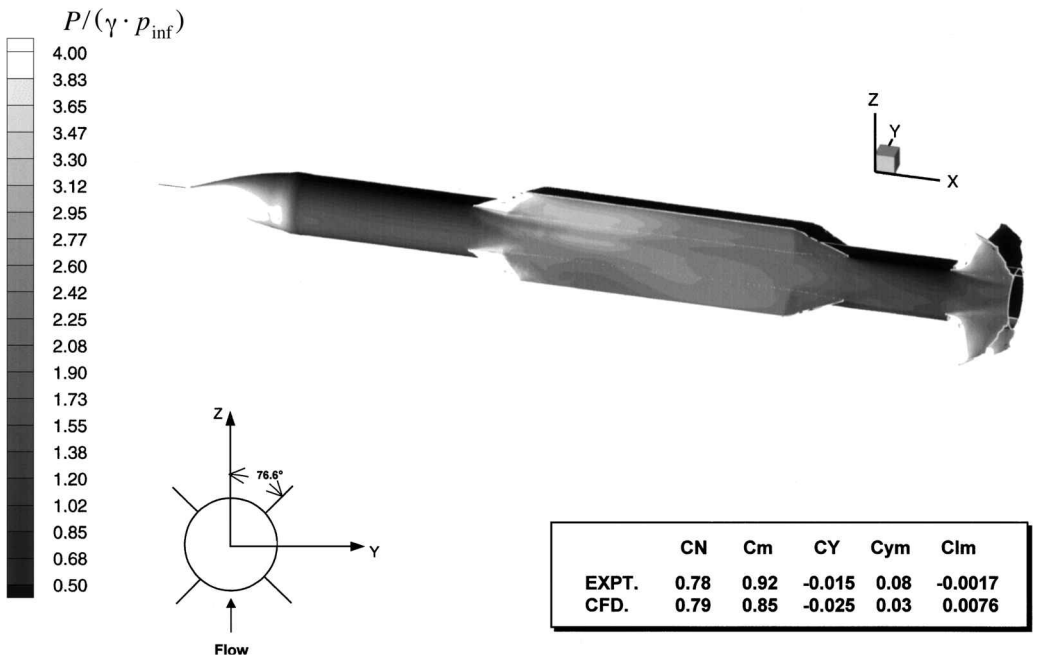

Fig. 12 Pressure distribution on missile surfaces for a supersonic asymmetric missile without jet: flow Mach number, 3.94; angle of attack, 3.1 deg; ϕ, 76.67 deg; and jet thrust, 50 lb.

compare reasonably well with the wind-tunnel data but not as well as earlier cases. Causes for such differences are unknown. However, for the next case, as shown in Fig. 6 at a lower angle of attack of 9.8 deg, the computational predictions are again in excellent agreement with the data. Similar comparisons are seen in Fig. 7, which is at a 3.1-deg angle of attack. Notice that the rolling-moment coefficient for this case is below the measurement accuracy and hence the comparisons for this coefficient are not suitable. CFD results for such cases are projected to be more reliable.

Test Cases Without Jets

Asymmetric Cases

We have wind-tunnel data for the nominal $M = 4.0$ without divert jets at several missile orientations and angles of attack. In an effort to establish a validation base, we picked cases at missile roll angles of nearly 76 and 109 deg at $\alpha = 20$, 10, and 3 deg. These cases are similar to jet cases. These results are shown in Figs. 8–12.

Figure 8 shows the computed results for a case with missile roll angle of 75.22 deg and $\alpha = 20$ deg without the divert jet. The computed pressure contours show high wing and tail loadings on the windward side, as anticipated. The overall comparison of the CFD predictions and the wind-tunnel data is excellent, as shown in the table in this figure.

Figure 9 shows a similar case for a missile roll angle of 109.42 deg at $\alpha = 20$ deg. Notice the excellent comparisons of the complete results with measurements. This case also can be compared with the case in Fig. 5 with a jet thrust of 50 lb. This comparison shows the effects of the jet interaction on the missile surface pressure distribution.

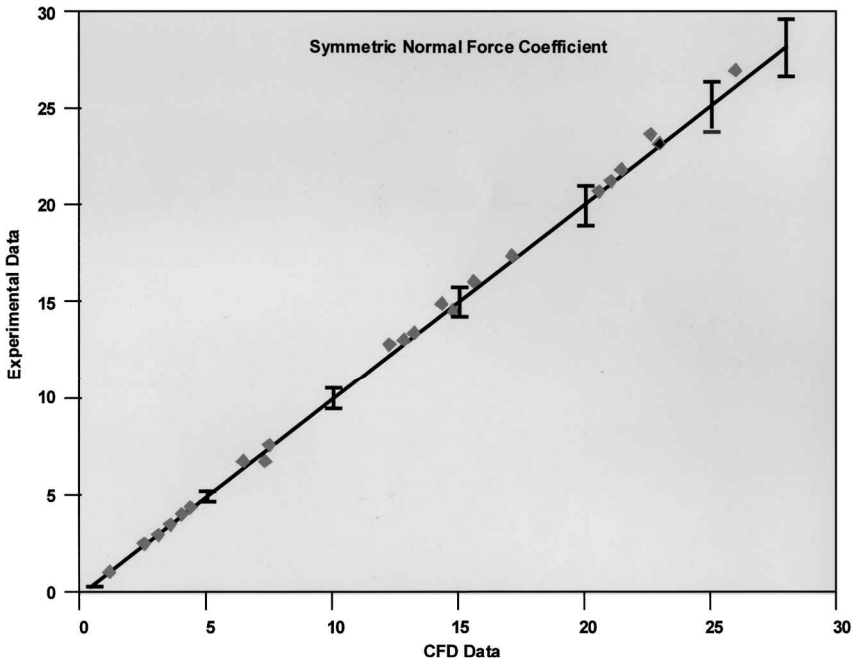

Fig. 13 Comparison of CFD and wind-tunnel measurements for a symmetric missile configuration: normal force coefficient.

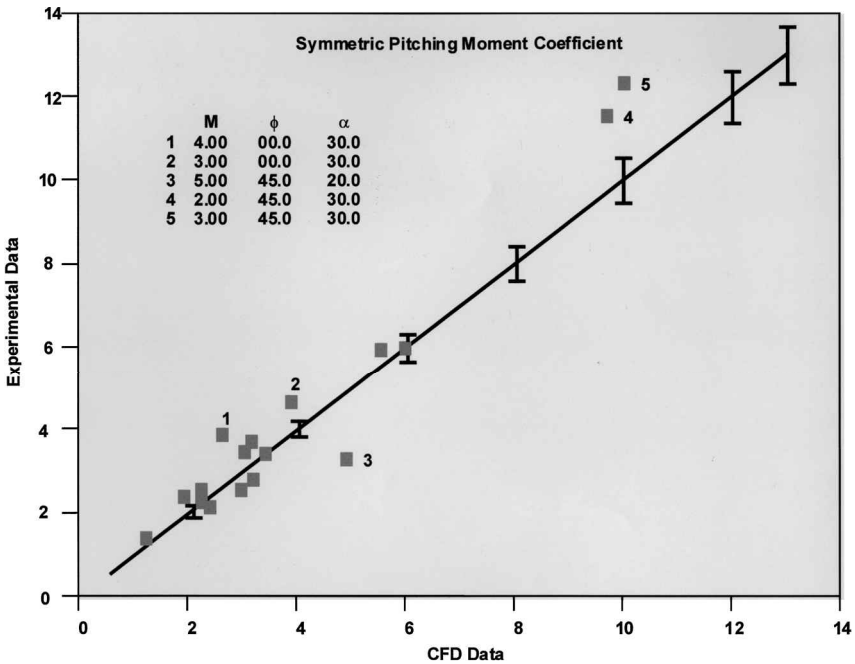

Fig. 14 Comparison of CFD and wind-tunnel measurements for a symmetric missile configuration: pitching moment coefficient.

Figure 10 shows a computation corresponding to the missile roll angle of 76.6 deg, as in Fig. 8, but at a lower angle of attack ($\alpha = 9.93$ deg), showing good comparisons with the data. A similar computational result is shown in Fig. 11 at a different roll angle of 110.7 deg at nearly the same angle of attack ($\alpha = 9.92$ deg), showing good comparisons with the data. Finally, Fig. 12 shows the result at a lower angle of attack ($\alpha = 3.1$ deg) but with a roll angle of 76.6 deg. Notice from these figures that the comparisons between the CFD predictions and the data deteriorate as the magnitudes of these quantities decrease. This observation is consistent with the measurement accuracy issues.

Symmetric Cases for $M = 2$, 3, and 5

Additional symmetric cases without jets were computed at several other Mach numbers, i.e., $M = 2.0$, 3.0, 4.0, and 5.0 for angles of attack up to 30 deg for the same missile geometry corresponding to a wind-tunnel test conducted at a different site. The computed and wind-tunnel normal force and moment coefficients are tabulated in Table 1 and plotted in Figs. 13 and 14. The computational results in these figures are plotted against the corresponding experimental values with a 45-deg line drawn to show differences between the two. Any deviation from this 45-deg line shows the degree of error between the two. These figures also contain an error bar representing ±5% of the local value. Notice from Fig. 13 that the normal force coefficients are predicted well within 5% of the wind-tunnel data. However, the pitching-moment coefficient, as seen in Fig. 14, shows larger-than-expected error. These differences are being examined primarily relative to the database from two different wind-tunnel tests and possible model differences.

Overall Asymmetric Results

As for the symmetric cases, all of the computational and experimental results for asymmetric cases can be put together in graphical and tabular forms, which are presented in Tables 2 and 3 and

Table 1 Comparison of normal-force and pitching-moment coefficients for symmetric cases (no jets)

				Comparison			
				CFD	Experimental	CFD	Experimental
Orientation	M	ϕ, deg	α, deg	C_N	C_N	C_m	C_m
+	5.00	0.00	30.0	12.23	12.83	3.10	3.68
X	5.00	45.00	20.0	6.41	6.71	4.87	3.28
X	5.00	45.00	15.0	4.31	4.33	3.13	2.79
X	5.00	45.00	10.0	2.52	2.52	2.15	2.22
X	5.00	45.00	5.0	1.13	1.05	1.16	1.41
+	5.00	0.00	35.0	15.58	16.10	2.91	4.27
+	4.00	0.00	10.0	3.01	2.94	1.87	2.37
+	4.00	0.00	30.0	13.23	13.40	2.55	3.87
+	2.00	0.00	30.0	17.10	17.33	5.50	5.94
+	2.00	0.00	10.0	4.00	4.05	2.32	2.15
+	3.00	0.00	30.0	14.36	14.88	3.83	4.62
+	3.00	0.00	10.0	3.52	3.52	2.18	2.50
X	2.00	45.00	30.0	14.74	14.49	9.70	11.51
X	2.00	45.00	10.0	3.48	3.47	3.37	3.42
X	3.00	45.00	30.0	12.82	13.05	10.05	12.33
X	3.00	45.00	10.0	3.17	3.13	2.99	3.44

Table 2 Comparison of force coefficient for asymmetric cases (with/without jets)

					Thurst ratio	Comparison			
						CFD	Experimental	CFD	Experimental
Orientation	M	ϕ, deg	α, deg	T, lb	$T/(qS_{\text{ref}})$	C_N	C_N	C_Y	C_Y
X	3.94	76.00	9.98	0.00	0.00	3.03	3.00	−0.13	−0.11
X	3.94	110.70	9.92	0.00	0.00	2.98	2.95	0.16	0.22
X	3.94	74.85	18.98	175.00	3.45	3.32	3.30	−2.25	−2.2
X	3.94	109.90	19.30	175.00	3.45	5.03	4.87	−3.5	−3.6
X	3.94	108.60	19.64	50.00	0.98	6.45	6.40	−0.88	−0.73
X	3.94	76.80	19.58	50.00	0.98	6.16	6.16	−0.95	−0.92
X	3.94	136.14	19.74	175.00	3.45	6.69	6.50	−4.03	−4.5
X	3.94	181.32	20.38	175.00	3.45	9.15	9.20	−2.3	−2.5
X	3.94	106.14	9.38	175.00	3.45	0.81	0.58	−3.4	−3.14
X	3.94	76.17	9.11	175.00	3.45	−0.69	−0.69	−2.15	−2.09
X	3.94	110.60	9.77	50.00	0.98	2.37	2.17	−0.98	−0.84
X	3.94	75.90	9.69	50.00	0.98	1.85	1.81	−0.76	−0.65
X	3.94	134.40	3.10	50.00	0.98	0.80	0.66	−1.16	−1.15
X	3.94	134.10	2.96	175.00	3.45	0.70	−0.05	−3.89	−3.91
X	3.94	74.40	2.28	175.00	3.45	−2.82	−2.93	−1.95	−1.6
X	3.94	76.60	3.12	0.00	0.00	0.79	0.78	−0.02	−0.02
X	3.94	133.30	3.12	0.00	0.00	0.75	0.77	0.0	0.02

Table 3 Comparison of moment coefficients for asymmetric cases (with/without jets)

					Thurst ratio,	Comparison					
						CFD	Experimental	CFD	Experimental	CFD	Experimental
Orientation	M	ϕ, deg	α, deg	T, lb	$T/(qS_{\text{ref}})$	C_m	C_m	C_{Ym}	C_{Ym}	C_{lm}	C_{lm}
X	3.94	76.00	9.98	0.00	0.00	1.91	2.18	0.38	0.51	−0.03	−0.05
X	3.94	110.70	9.92	0.00	0.00	2.08	2.32	−0.43	−0.46	0.05	0.04
X	3.94	74.85	18.98	175.00	3.45	−6.84	−6.56	−4.62	−3.93	−0.27	−0.27
X	3.94	109.90	19.30	175.00	3.45	−1.87	−1.72	−10.90	−11.09	0.44	0.47
X	3.94	108.60	19.64	50.00	0.98	1.71	2.22	−3.85	−4.01	0.39	0.40
X	3.94	76.80	19.58	50.00	0.98	−0.11	0.65	−0.89	−0.47	−0.31	−0.26
X	3.94	136.14	19.74	175.00	3.45	5.05	5.03	−12.00	−12.26	0.34	0.26
X	3.94	181.32	20.38	175.00	3.45	13.85	13.92	−10.03	−10.37	0.43	0.43
X	3.94	106.14	9.38	175.00	3.45	−4.15	−4.92	−10.66	−9.89	0.14	0.14
X	3.94	76.17	9.11	175.00	3.45	−8.35	−8.35	−5.90	−5.09	0.02	−0.04
X	3.94	110.60	9.77	50.00	0.98	0.43	0.51	−3.60	−3.66	0.11	0.18
X	3.94	75.90	9.69	50.00	0.98	−1.19	−0.66	−1.52	−1.26	−0.02	0.03
X	3.94	134.40	3.10	50.00	0.98	0.81	0.65	−3.98	−3.84	0.01	0.04
X	3.94	134.10	2.96	175.00	3.45	0.51	−1.58	−12.37	−12.03	0.03	0.06
X	3.94	74.40	2.28	175.00	3.45	−9.93	−10.16	−5.89	−4.83	0.00	0.02
X	3.94	76.60	3.12	0.00	0.00	0.83	0.92	−0.03	0.08	0.01	0.00
X	3.94	133.30	3.12	0.00	0.00	0.91	0.98	0.01	−0.02	0.01	0.00

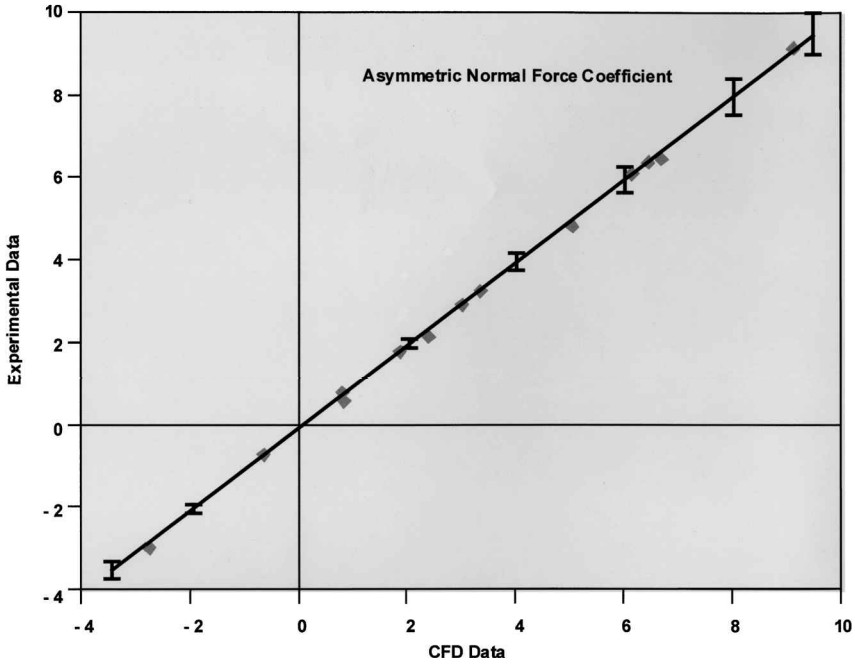

Fig. 15 Comparison of CFD and wind-tunnel measurements for an asymmetric missile configuration: normal force coefficient.

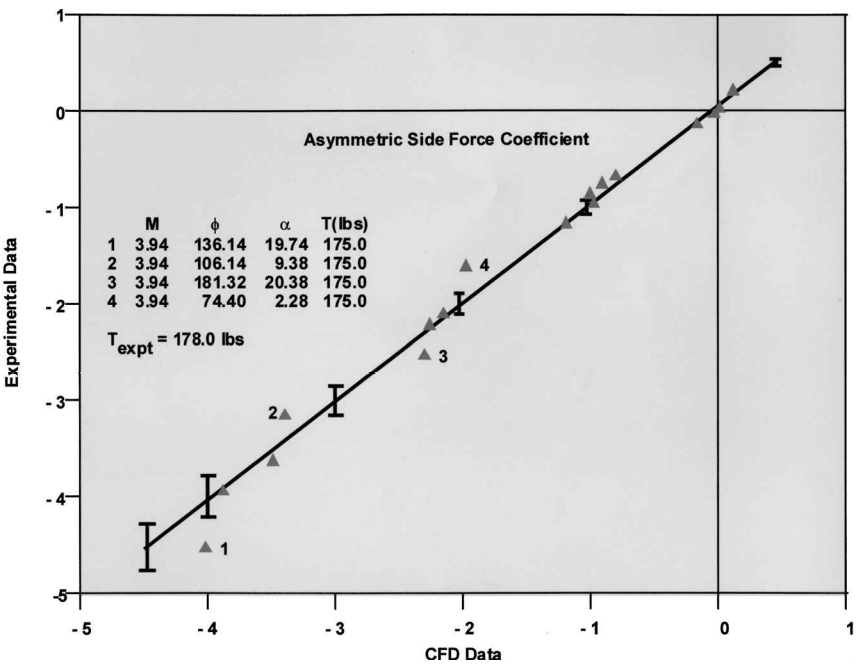

Fig. 16 Comparison of CFD and wind-tunnel measurements for an asymmetric missile configuration: side force coefficient.

Figs. 15–19. The computational results in these figures are again plotted against the corresponding experimental values with a 45-deg line drawn to show differences between the two. Any deviation from this 45-deg line shows the degree of error between the two. These figures also contain an error bar representing ±5% of the local value. These results show an excellent comparison of the computed results with the wind-tunnel data, close to ±5%. There are isolated points in all figures that give larger than ±5% error between CFD predictions and the wind-tunnel data, as is seen from these figures, but there appears to be no pattern to these differences. However, the overall results show excellent predictive ability of the CFD approach with and without divert jets at several angles of attack and roll angles. Notice also that these results for the moment predictions are significantly better than the symmetric cases discussed earlier.

Discussion

The preceding results encompass a large number of cases with and without jets at several angles of attack and missile roll angles. All of these computed cases show excellent agreement with the wind-tunnel data, allowing us to develop an understanding of the jet interaction process by examining the complex details of the computed flowfield. Some of these conclusions are outlined next.

Effect of Roll Angle

Previous efforts[1,4] have discussed the jet interaction process as the missile is rolled to move the divert jet from the leeward plane to windward plane (only symmetric cases were computed before). Using the current full asymmetric simulations, those observations now can be confirmed:

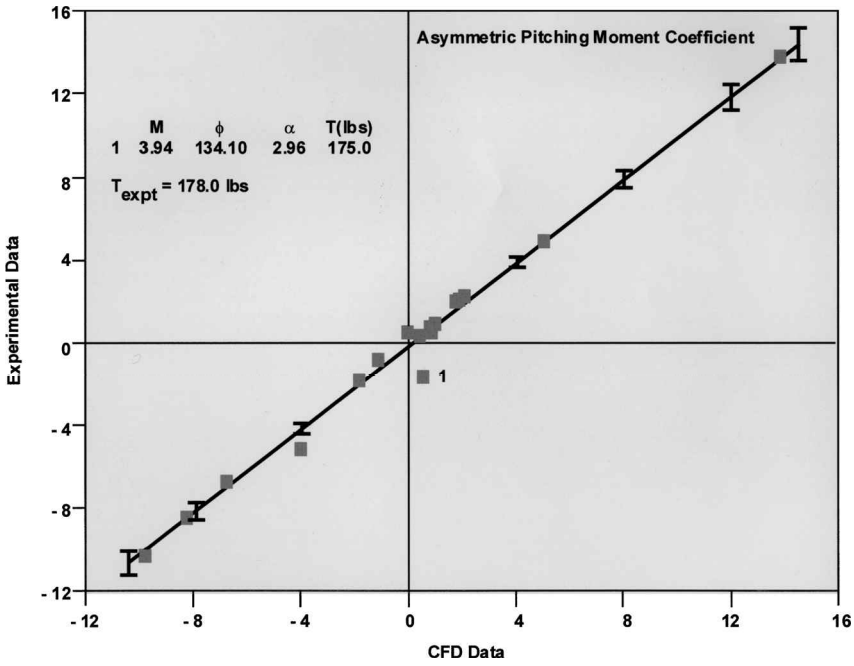

Fig. 17 Comparison of CFD and wind-tunnel measurements for an asymmetric missile configuration: pitching moment coefficient.

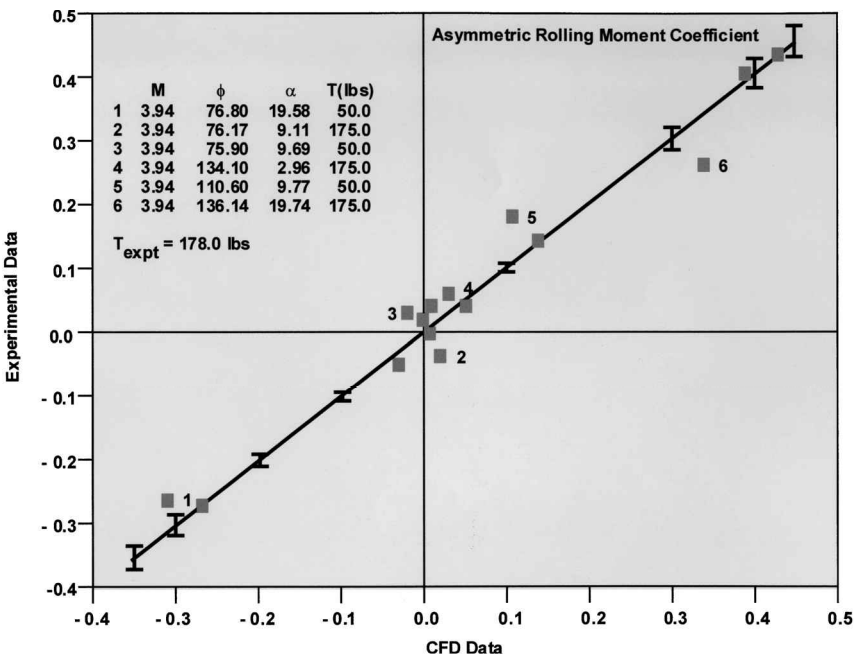

Fig. 18 Comparison of CFD and wind-tunnel measurements for an asymmetric missile configuration: rolling moment coefficient.

1) The normal-force amplification factor $[1 + (C_{N_{\text{jet}}} - C_{N_{\text{no-jet}}})/(T/q \cdot S)]$ reduces to a very low value as the missile is rolled to bring the divert jet from the leeward to the windward side. This process is reversed as the roll continues to bring the divert jet from the windward to the leeward side.

2) The physical effects that cause these phenomena are as follows: a) Blockage effect of the jet on the windward side that wipes out the windward wing and tail panel loadings. The degree of blockage is dependent on the azimuthal location of the jet on the missile body. b) Jet wraparound effect that produces unfavorable pressure on the opposite side of the missile body and lifting surfaces. These effects can be reduced by multiple jets on the missile body but their magnitude is small compared to the effect described in item (a). c) Favorable high-intensity pressure zone ahead of the divert jet is very narrow to circumvent the negative effects outlined above.

Jet Location Selection

Jet location selection, to alleviate low force amplification factor in windward orientation, is an important design parameter for the enhancement of missile performance. On the basis of the studies presented, wing panels forward of the divert jet alleviate the force amplification factor but only at the cost of lost tail effectiveness (see Ref. 4 for more details). We propose wingtip-mounted divert jets to alleviate all aerodynamic problems. This, however, requires an appropriate engineering development to address packaging and structural integrity issues.

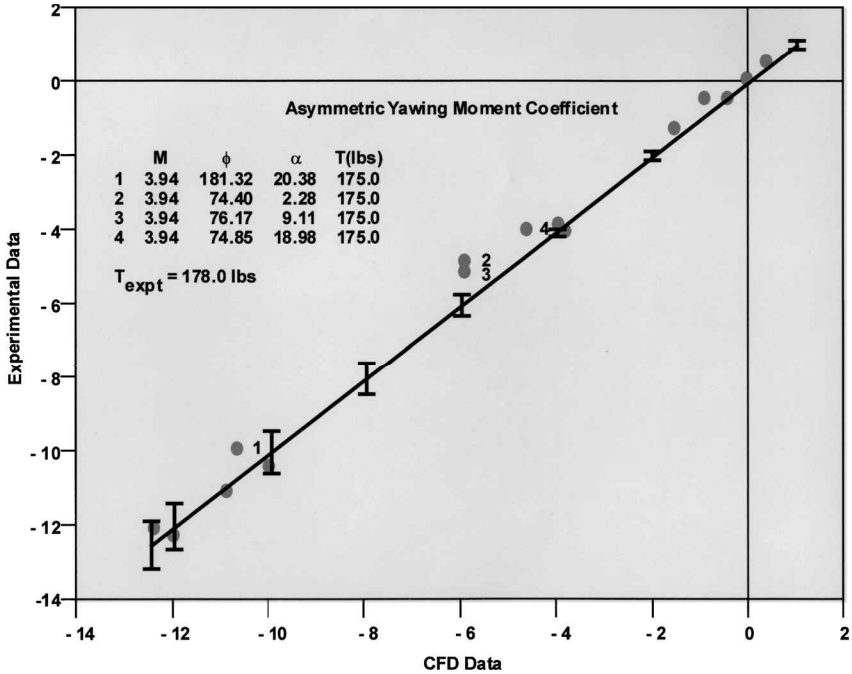

Fig. 19 Comparison of CFD and wind-tunnel measurements for an asymmetric missile configuration: yawing moment coefficient.

Conclusions

Asymmetric missile configuration at a nominal-flow Mach number of 4.0, angles of attack ranging from 3 to 30 deg, and several missile roll angles with and without divert jets are studied using FNS computational methodology to show excellent agreement of the predicted force and moment coefficients with the available wind-tunnel data. On the basis of these studies, several earlier observations of the jet interaction effects based on symmetric CFD simulations are confirmed. Additionally, CFD-computed results were examined to first determine the causes and then to recommend means to alleviate the low force amplification factors observed for windward-oriented jets.

References

[1]Srivastava, B. N., "Lateral Jet Effectiveness Studies for a Missile Using Navier–Stokes Solutions," 5th Annual AIAA/BMDO Technology Readiness Conference and Exhibit, Paper 11-08 alt, Eglin Air Force Base, Ft. Walton Beach, FL, Sept. 1996.

[2]Srivastava, B. N., "Lateral Jet Control of Supersonic Missile: CFD Predictions and Comparisons to Force and Moment Measurements," *Journal of Spacecraft and Rockets*, Vol. 35, No. 2, 1997, pp 140–146.

[3]Srivastava, B. N., "CFD Analysis and Validation for Lateral Jet Control of a Missile," *Journal of Spacecraft and Rockets*, Vol. 34, No. 5, 1997, pp. 584–592.

[4]Srivastava, B. N., "Aerodynamic Performance of Supersonic Missile Body- and Wing Tip-Mounted Lateral Jets," *Journal of Spacecraft and Rockets*, Vol. 35, No. 3, 1998, pp. 278–286.

[5]Cassel, L. A., Davis, J. G., and Engh, D. P., "Lateral Jet Control Effectiveness Prediction for Axisymmetric Missile Configurations," U.S. Army Missile Command, Rept. RD-TR-68-5, Redstone Arsenal, AL, June 1968.

[6]Spring, D., "An Experimental Investigation of the Interference Effects Due to a Lateral Jet Issuing from a Body of Revolution over the Mach No. Range of 0.8 to 4.5," U.S. Army Missile Command, Rept. RD-TR-68-10, Redstone Arsenal, AL, Aug. 1968.

[7]Chamberlain, R., "Control Jet Interaction Flowfield Analysis," *Aerodynamic Investigations*, Lockheed, Rept. LMSC F268936, Vol. 5, Feb. 1990.

[8]Chamberlain, R., "Calculation of Three-Dimensional Jet-Interaction Flowfields," AIAA Paper 90-2099, 1990.

[9]Weatherly, D., and McDonough, J., "Performance Comparisons of Navier–Stokes Codes for Simulating Three-Dimensional Hypersonic Crossflow/Jet Interaction," AIAA Paper 91-2096, 1991.

[10]York, B. J., Sinha, N., Kenzakowski, D. C., and Dash, S. M., "PARCH Code Simulation of Tactical Missile Plume/Airframe/Launch Interactions," 19th JANNAF Exhaust Plume Technology Meeting, CPIA PWB 568, 1991, pp. 645–674.

[11]Chan, S. C., Roger, R. P., Edwards, G. L., and Brooks, W. B., "Integrated Jet Interactions, CFD Predictions, and Comparison to Force and Moment Measurements for a Thruster Attitude Controlled Supersonic Missile," AIAA Paper 93-3522, 1993.

[12]Lytle, J. K., Harloff, G. J., and Hsu, A. T., "Three-Dimensional Compressible Jet-in-Crossflow Calculations Using Improved Viscosity Models and Adapted Grid," AIAA Paper 90-2100, 1990.

[13]Dash, S. M., Sinha, N., York, B. J., Lee, R. A., and Hosangadi, A., "On the Inclusion of Advanced Turbulence Models and Nonequilibrium Thermochemistry into State-of-the-Art CFD Codes and Their Validation," AIAA Paper 92-2764, 1992.

[14]Rizzetta, D. P., "Numerical Simulation of Slot Injection into a Turbulent Supersonic Stream," AIAA Paper 92-0827, 1992.

[15]Darmieux, M., and Marasaa-Poey, R., "Numerical Assessment of Aerodynamic Interactions on Missiles with Transverse Jets Control," AGARD Meeting on Computational and Experimental Assessment of Jets in Cross Flow, April 1993.

[16]Dash, S. M., York, B. J., Sinha, N., Lee, R. A., Hosangadi, A., and Kenzakowski, D. C., "Recent Developments in the Simulation of Steady and Transient Transverse Jet Interactions for Missile, Rotorcraft, and Propulsive Applications," AGARD Meeting on Computational and Experimental Assessment of Jets in Cross Flow, April 1993.

[17]Chan, S. C., Roger, R. P., Brooks, W. B., Edwards, G. L., and Boukather, S. B., "CFD Predictions and Comparisons to Wind Tunnel Data for the Asymmetric Firing of a Forward Mounted Attitude Control Thruster," AIAA Paper 95-1895, June 1995.

[18]Qin, N., and Foster, G. W., "Study of Flow Interactions Due to a Supersonic Lateral Jet Using High Resolution Navier–Stokes Solutions," AIAA Paper 94-2151, June 1994.

[19]Steinbrenner, J. P., and Chawner, J. R., "Recent Enhancements to the GRIDGEN Structural Grid Generation System," *Proceedings of the NASA Workshop on Software Systems for Surface Modeling and Grid Generation*, NASA, 1992.

R. M. Cummings
Associate Editor